Journal of Membrane Science 333 (2009) 88–93

Contents lists available at ScienceDirect

Journal of Membrane Science

journal homepage: www.elsevier.com/locate/memsci

High permeable PTMSP/PAN composite membranes for solvent nanofiltration

Alexey V. Volkov[a,*], Victor V. Parashchuk[a], Dimitris F. Stamatialis[b], Valery S. Khotimsky[a], Vladimir V. Volkov[a], Matthias Wessling[b]

[a] Topchiev Institute of Petrochemical Synthesis RAS, Leninsky pr. 29, 119991, Moscow, Russia
[b] IMPACT Research Institute, Faculty of Science and Technology, Membrane Technology Group, University of Twente, P.O. Box 217, NL-7500 AE, Enschede, The Netherlands

ARTICLE INFO

Article history:
Received 25 November 2008
Received in revised form 23 January 2009
Accepted 31 January 2009
Available online 10 February 2009

Keywords:
PTMSP
Composite membrane
Nanofiltration
Solvents
PAN

ABSTRACT

This paper describes the preparation of composite membranes comprising a poly[1-(trimethylsilyl)-1-propyne] (PTMSP) top-layer on a porous poly(acrylonitrile) (PAN) support. The PTMSP layer has different top-layer thickness in the range of 0.7–6.3 μm. The optimized PTMSP/PAN composite membranes with top-layer thickness of about 1 μm have ethanol permeability of 3.8 kg/(m^2 h bar) and 90% retention of the negatively charged dye Remazol Brilliant Blue R (MW 626.5) at 5 bar. The permeability of methanol, ethanol or acetone through the PTMSP/PAN composite membranes is higher than a number of commercial available nanofiltration membranes, whereas all membranes have rejection of about 90% for negative charged dyes of different molecular weight. The permeability of methanol, ethanol and acetone through the PTMSP/PAN composite membranes depends on solvent viscosity and membrane swelling; the solvent viscosity seems to be the dominant factor.

1. Introduction

Organic Solvent Nanofiltration (OSN), or Solvent Resistant Nanofiltration (SRNF), is a rapidly growing area of membrane technology due to its great potential and advantages over the traditional separation methods such as distillation or extraction. In some cases (e.g. solvent exchange in multistage synthesis with thermally unstable intermediates [1]), OSN can be considered unique separation process that could provide effective and almost quantitative recovery of target compounds in different areas, including chemical, petrochemical and food industries [2].

Key part of the OSN process is a membrane which should be stable in organic media, show high permeability for selected solvents and possess high retention of target compounds. In contrast to the nanofiltration of aqueous systems that has many decades of history, nanofiltration membranes for organic media are still limited in number. The existing polymeric membranes can be divided into three groups: elastomeric/rubbery polymers, conventional glassy polymers and high free volume glassy polymers.

To increase the mechanical stability of elastomeric polymers (e.g. silicone rubbers, polyurethanes, etc.) in solvents and achieve high retention of target compounds, these polymers are often cross-linked [3,4]. Besides, the addition of fillers (e.g. zeolites in PDMS [5,6]) also increases the membrane stability and improves membrane retention in polar and non-polar solvents. The membrane selectivity is determined by difference in solubility and diffusivity of the components the mixture to be separated. Nonetheless, other parameters, such as dragging (coupling) may also effect the membrane transport and selectivity [7]. These are usually composite type nanofiltration membranes based on nonporous top-layer on a support.

For conventional glassy polymers (polyamides, polyimides, polysulfones, etc.), the nanoporous structure of selective layer is mainly created by immersion precipitation, although recently, the interfacial polymerization has also been used [8]. In contrast to elastomeric membranes, the membrane selectivity is often determined by the difference in size of the molecules to be separated. Nonetheless, the membrane–solvent–solute interactions may also play a major role in transport [9]. To increase the solvent resistance of some of these membranes in wider range of solvents including DMF, NMP, DMAc, DMSO, etc. the membranes are cross-linked post-membrane formation (e.g. polyimides Lenzing P84 [10] or Matrimid® [11]).

In earlier work some of the authors proposed using poly[1-(trimethylsilyl)-1-propyne] (PTMSP) for the preparation of OSN membranes [12–14]. PTMSP is a hydrophobic glassy polymer (T_g > 300 °C) with extremely high free volume fraction (up to 25%) that provides the highest gas permeability among the known poly-

* Corresponding author. Tel.: +7 495 955 4293; fax: +7 495 633 8520.
E-mail address: avolkov@ips.ac.ru (A.V. Volkov).

0376-7388/$ – see front matter © 2009 Elsevier B.V. All rights reserved.
doi:10.1016/j.memsci.2009.01.050

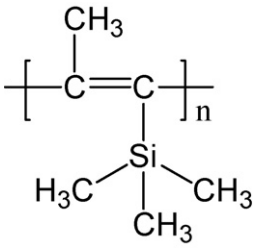

Fig. 1. The structure of poly[1-(trimethylsilyl)-1-propyne] (PTMSP).

mers [15]. The intrinsic nanoporous structure of PTMSP is naturally formed during the casting of polymeric solution and no subsequent treatment is required. It is stable in alcohols, ketones and some aliphatic hydrocarbons (PTMSP with *cis*-conformation higher than 65% is insoluble in hexane and heptane [16]). In our previous work [12], it was shown that dense PTMSP membranes with thickness of 24–30 μm have high ethanol permeability exceeding those of commercially silicone-based membranes (MPF-50 and Membrane D). In this work, the development of a composite membranes with PTMSP selective layer onto a commercial poly(acrylonitrile) (PAN) porous support is investigated. The transport properties of these membranes are systematically studied including permeation of various pure solvents (methanol, ethanol, acetone) and the retention of a negatively charged dye Remazol Brilliant Blue R (MW 626.5).

2. Experimental

2.1. Chemicals

The following chemicals were used as received: methanol (Chimmed), ethanol (Acros Organics or Chimmed), acetone (Chimmed), chloroform (Chimmed), cyclohexane (Fluka) and Remazol Brilliant Blue R (Acros Organics).

2.2. Membrane preparation

To develop composite membranes with thin top-layer, PTMSP polymer (Fig. 1) with high molecular weight was used (catalytic system: $TaCl_5$/Al(*i*-Bu)$_3$, $[TMSP]_o = 0.75$ M, $[TMSP]/[TaCl_5] = 100$, $[Al(i\text{-}Bu)_3]/[TaCl_5] = 0.3$, solvent: toluene, $T = 25\,^{\circ}C$; $M_w = 2{,}000{,}000$, $M_w/M_n = 3.7$; $[\eta] = 6.0$ dl/g, $\rho = 0.789$ g/cm^3; *cis*/*trans* ratio: 45/55). The PAN porous support (HV-II, MWCO 50 kDa; kindly supplied by GKSS) has good solvent stability [17] and has already been used for OSN membranes [3,4,18–23]. It was previously reported [24] that dense PTMSP membranes (catalyst: $TaCl_5$) simultaneously possess higher gas permeability, selectivity and free volume fraction in the following order of the casting solvents: cyclohexane > toluene > THF. Therefore, cyclohexane was used as a casting solvent for PTMSP.

Prior to PTMSP casting, all dusts were removed from the surface of PAN-support, fixed with tape on glass plate (20 cm × 35 cm), by air stream. After membrane casting at ambient conditions (see details in Table 1), the glass plate with fixed composite membrane was placed in fume hood to complete solvent evaporation. Then, the PTMSP/PAN membrane was taken off the plate and was stored in corresponding solvent (methanol, ethanol or acetone) prior to the filtration testing. Four membrane coupons were cut from the same PTMSP/PAN composite membrane sample and placed into the permeation cells in swollen state for the permeation experiments. Besides, dense PTMSP-membranes (catalytic system: $TaCl_5$/Al(*i*-Bu)$_3$ or $NbCl_5$ [12]) were cast from 1 wt.% cyclohexane solution onto cellophane. Before the filtration, all dense membranes ($TaCl_5$/Al(*i*-Bu)$_3$) were soaked in ethanol overnight at room temperature and atmospheric pressure.

Table 1
Casting conditions of PTMSP/PAN composite membrane.

Membrane sample	Casting conditions		
	C_{PTMSP} (wt%)	Casting knife (mm)	Number of layers
PTMSP-1	1.0	0.20	1
PTMSP-2	0.7	0.20	1
PTMSP-3	0.5	0.20	1
PTMSP-4	0.3	0.20	1

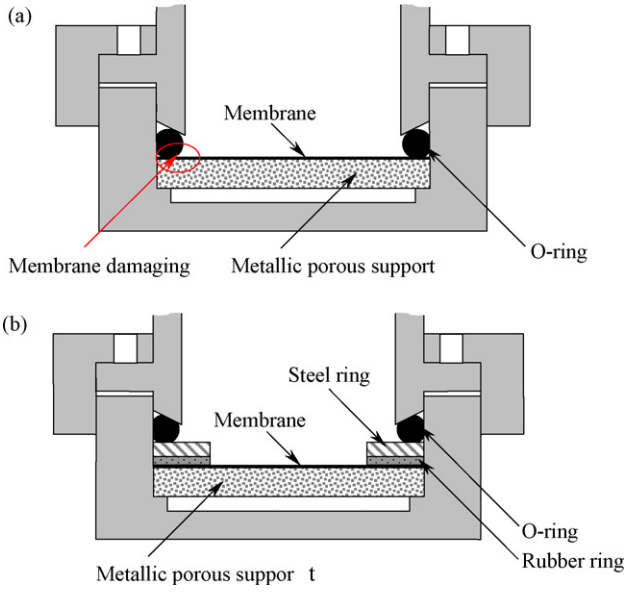

Fig. 2. Scheme of dead-end nanofiltration cell used in this study (stirring bars are not presented here): (a) "standard" membrane sealing with O-rings, (b) optimized membrane sealing.

2.3. The filtration set-up

Testing of PTMSP/PAN composite membranes and dense samples was carried out in two dead-end filtration cells. Fig. 2 shows the schemes of the initial dead-end cell (3.32×10^{-3} m^2) and after membrane sealing optimization (1.96×10^{-3} m^2). All cells were equipped with magnetic stirring bar to minimize the concentration polarization. Helium was used to pressurize the liquid above the membrane [12]. The permeate collector was arranged in such a way to minimize the evaporation of ethanol during testing. All filtration experiments were carried out at $23 \pm 2\,^{\circ}C$ and trans-membrane pressure up to 20 bar. All reported results are averages obtained using at least two different membrane samples. The maximum difference in the permeability of the samples cast at the same conditions was less than 15%.

2.4. Retention studies

For retention experiments the negatively charged dye Remazol Brilliant Blue R (MW 626.5) was used due to absence any specific interaction with PTMSP material [12]. The feed dye solution concentration was 15 mg/l. The dye concentration analysis was performed using UV–vis spectrophotometer Spekol 11 ($\lambda_{max} = 582$ nm). For methanol, ethanol and acetone dye solutions, the calibration line was linear in the concentration range of 0–54 mg/l. The dye retention values by the membranes were calculated using the following

equation:

$$R(\%) = \left(1 - \frac{C_{ip}}{C_{if}}\right) \cdot 100\% \quad (1)$$

where C_{ip}, C_{if} is the dye concentration (g/g) in the permeate and the feed, respectively. For every simple experiment the dye concentration in the feed was recalculated with respect to mass balance and initial dye concentration; these calculations were verified by experimental measurements of the dye concentration in the feed before and after the filtration. During the dead end filtration experiments, the dye concentration in the feed was increased up to 35% in comparison to the initial value. The maximum difference in retention of PTMSP/PAN composite membrane cast at same conditions was less than 4%.

2.5. Swelling experiments

Dense PTMSP membrane samples with diameter of 50 mm and thickness of 100 μm were used for the swelling experiments in various solvents. Soaking in methanol, ethanol and acetone was carried out for 2 days where swelling equilibrium was reached. After removal of excess solvent from the membrane surface, the membrane size and weight were measured. The swelling degree, SD, was calculated using the following equation:

$$SD = \frac{d_s \cdot r_s^2 - d_0 \cdot r_0^2}{d_0 \cdot r_0^2} \quad (2)$$

where d_0, d_s is thickness of initial and swollen membrane, respectively [m]; r_0, r_s is radius of initial and swollen membrane, respectively [m].

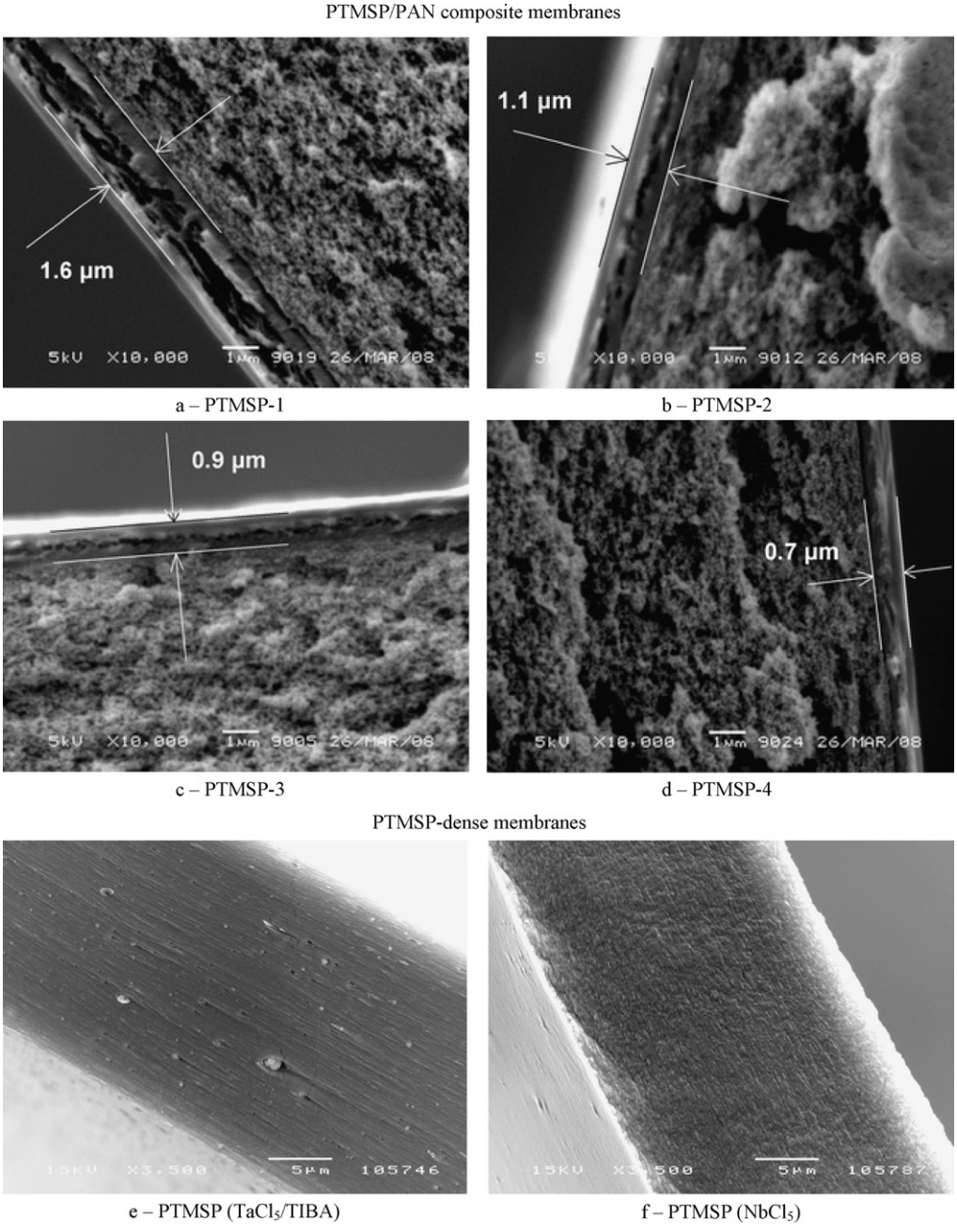

Fig. 3. Membranes cross-section visualized by SEM analysis.

Table 2
Estimation of dry thickness of PTMSP-layer in composite membranes.

PTMSP sample	Estimated PTMSP-layer thickness (μm)	
	SEM	Ethanol permeability
PTMSP-1	1.6 ± 0.1	1.1 ± 0.2
PTMSP-2	1.1 ± 0.1	0.8 ± 0.2
PTMSP-3	0.9 ± 0.1	0.6 ± 0.1
PTMSP-4	0.7 ± 0.1	0.5 ± 0.1

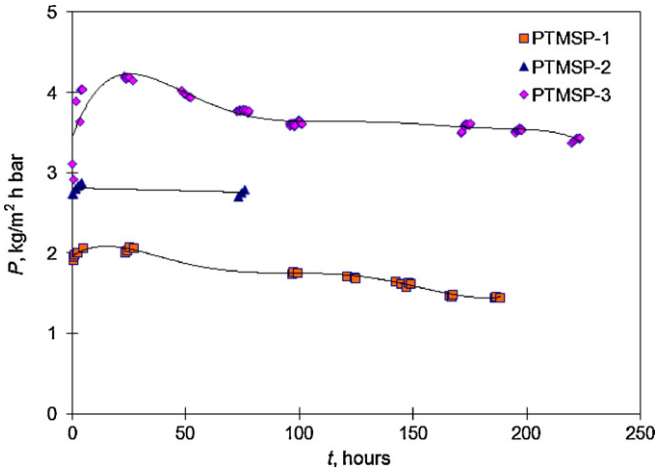

Fig. 4. Time stability test: ethanol permeability at trans-membrane pressure of 5 bar (samples: PTMSP-8, PTMSP-9 and PTMSP-10).

2.6. SEM visualization

The membrane morphology was characterized by Scanning Electron Microscopy (SEM, Microscope Jeol JSM-5600LV, at 5–15 kV). The samples were broken in liquid nitrogen and sputtered with gold under vacuum for 300 s at a current of 15 mA.

3. Results and discussions

3.1. Estimation of PTMSP-layer thickness in the composite membranes

Table 2 presents estimation of the thickness of the PTMSP-layer of the composite membranes based on two methods: (i) SEM visualization and (ii) normalized ethanol permeability.

In the first method, the PTMSP layer thickness was estimated from the membrane cross-section obtained by SEM (see Fig. 3a–d; the "cracks" in this images are due to sample breaking in liquid nitrogen). In contrast to dense samples of PTMSP ($TaCl_5$/TIBA; Fig. 4e), the PTMSP with higher *cis*-fraction of macromolecular chains ($NbCl_5$; *cis*/*trans* ratio: 63/37) have "uniform" morphology (Fig. 3f) in agreement to the literature [25,26].

In the second method, the top-layer thickness of the composite membranes was recalculated from their ethanol permeability by using an average of normalized ethanol permeability, 2.1×10^{-6} kg m/(m^2 h bar), through three different dense PTMSP membranes ($TaCl_5$/TIBA) with thickness of 21 ± 1 μm. For these estimations, we assumed a linear relationship between solvent transport across the membrane and selective layer thickness and that pore intrusion does not affect the ethanol transport through PTMSP. Table 2 shows that the top-layer thickness for the membranes estimated from ethanol permeability agrees well that estimated via SEM suggesting that probably PTMSP intrusion in the PAN is very small.

Table 3
Nanofiltration characteristics of PTMSP/PAN composite membranes.

PTMSP sample	PTMSP layer thickness	Ethanol permeability[a] (kg/(m^2 h bar)) (Retention[a], %)		
		5 ± 1 bar	10 ± 1 bar	20 ± 1 bar
PTMSP-1[b]	1.6	–	3.8 (2)	–
PTMSP-1	1.6	2.0 (94)	2.0 (–)	2.0 (–)
PTMSP-2	1.1	2.8 (92)	–	–
PTMSP-3	0.9	3.8 (90)	3.6 (–)	2.9 (–)
PTMSP-4	0.7	4.6 (79)	–	–

[a] Average values of at least two different membrane samples.
[b] Standard O-ring sealing.

3.2. Nanofiltration performance of PTMSP/PAN composite membranes

During initial optimization experiments it was found that relatively high polymer concentration (at least 4.1 wt.% or higher) leads to delaminating of PTMSP-layer from PAN-support when the membrane is soaked in ethanol. The dense PTMSP membranes swell in ethanol about 63 ± 4%, whereas the swelling of PAN-support is almost negligible in this solvent. It seems that due to high PTMSP-solution viscosity at high polymer concentration there is not sufficient pore intrusion of polymeric solution into the support to achieve integration between PTMSP layer and PAN-support. Further decreasing of PTMSP concentration to 2.4 wt.% or lower increases pore intrusion. Then, the produced membranes do not delaminate in ethanol, methanol and acetone.

Initially, PTMSP/PAN composite membranes were tested in the dead-end filtration cell with "standard" sealing, where the O-ring is in direct contact to the membrane. In these experiments the membranes had extremely low dye retention (see PTMSP-1[b] in Table 3). Careful inspection of the membranes after filtration reveals blue spots or even a circle on the top of the PAN-support. Those are mainly observed in the area where sealing O-ring contacts the membrane (see Fig. 2a). It seems that the O-ring damages the PTMSP layer causing leakage through the membrane. At the same time, this problem did not arise for the PTMSP dense membranes due to its high thickness [12] and for the PDMS/PAN composite membranes (top-layer thickness of 2 μm) due to its high cross-linking degree and sufficient pore intrusion [3–4,7].

In the literature, lower retention than expected has also been reported for commercial membranes STARMEM (dead-end cell with O-rings) [27]. The authors there attributed the low retention to

Table 4
Comparison of nanofiltration characteristics (solvent permeability [*P*, kg/(m^2 h bar)] and solute rejection [*R*, %]): PTMSP/PAN composite membranes (this work) and commercial OSN-membranes [30].

Membranes	$P_{methanol}$ (kg/(m^2 h bar))	R_{S1} (%)	R_{S2} (%)	$P_{ethanol}$ (kg/(m^2 h bar))	R_{S1} (%)	R_{S2} (%)	$P_{acetone}$ (kg/(m^2 h bar))	R_{S1} (%)	R_{S2} (%)
Desal-5-DK	0.4	99	–	0.2	79	–	–	–	–
MPF-44	1.5	93	–	1.1	92	–	0.6	84	–
MPF-50	2.0	97	–	0.9	92	–	1.7	93	–
SolSep-169	38.0	72	–	25.2	86	–	31.6	91	–
PTMSP/PAN	**6.1**	**–**	**90**	**3.8**	**–**	**90**	**13.6**	**–**	**85**

S1: Erythrosine B (MW 880; negative charged); S2: Remazol Brilliant Blue R (MW 626.5; negative charged).

Table 5
Solvent viscosities, molar volume and experimental data for swelling degree of PTMSP membranes.

Solvent	Solvent properties			Membrane–solvent interaction	
	Dynamic viscosity of solvent μ (cP)	Kinematic viscosity of solvent ν (St)	Molar volume V_m (cm^3/mol)	Sorption (mol/mol)	Swelling SD
Methanol	0.54	6.83	40.4	2.2 ± 0.1	0.42 ± 0.04
Ethanol	1.08	13.69	58.4	2.4 ± 0.1	0.63 ± 0.04
Acetone	0.30	3.79	73.3	1.4 ± 0.1	0.53 ± 0.04

"a leak flux" defects in the membrane (including the case of possible membrane damaging by O-ring) or around the sealing.

To avoid damaging the thin PTMSP layer during testing, the dead-end filtration cells were optimized by introducing two additional rings (stainless steel and cross-linked silicone rubber material; see Fig. 2b). An O-ring is still used for sealing but the force on the membrane is distributed on much bigger membrane area in comparison with "standard" sealing. These cross-linked silicone rubber rings prevent membrane damage even at high pressure without any effect on the membrane permeation; after soaking them in 100 ml of ethanol dye solution for 6 h there was no significant dye adsorption. Further testing of membranes was carried out with this optimized sealing. Table 3 shows that the average value of dye retention for samples of PTMSP-1, PTMSP-2 and PTMSP-3 is 94, 92 and 90% at 5 bar, respectively, which is comparable with that of dense PTMSP-membranes (~94%) [12]. It seems that the optimized sealing allows us to characterize high permeable OSN-membranes without damaging during the operation. Further decrease of the polymer casting solution concentration to 0.3 g/l (PTMSP-4) leads to lower retention (R = 79%) probably due to membrane defects (low top-layer thickness). It seems that the optimal casting conditions are: polymer concentration of 0.5 g/l, with casting knife is 0.20 mm. The obtained membranes have ethanol permeability of about 3.8 kg/(m^2 h bar) and dye retention 90% at 5 bar (see PTMSP-4 in Table 2).

The PTMSP-3 membranes with selective layer thickness of 0.9 μm suffer reversible compaction when the applied pressure increases from 5 to 20 bar and then decreases back to 5 bar, while the PTMSP-1 thicker membrane (top layer thickness 1.6 μm) shows no compaction (see Table 3). Perhaps the "bulk" membrane properties (e.g. mechanical stability) may not be completely realized in the very thin selective layer of PTMSP-3 due to possible derivation in the macromolecules packaging, which may easily take place in the boundary region of the membrane. Membrane compaction often occurs and is widely reported in the literature (tailor-made cross-linked polyurethanes (selective layer: 3.0 μm) [23] or cross-linked silicone rubber (MPF-50; selective layer: 0.1 μm) [28]).

Fig. 4 presents pure ethanol permeability for the PTMSP-1, PTMSP-2 and PTMSP-3 at 5 bar for filtration up to 200 h showing that these membranes show quite good stability with slight decrease of ethanol transport during the testing period. Thin PTMSP membranes show accelerating physical aging in gas permeation testing [29] – nitrogen and helium permeability through 1 μm membrane decline about 4 times after 200 h of testing, while thick PTMSP sample (85 μm) possesses stable permeability of these two gases [29]. In OSN no such decline is observed for the PTMSP/PAN composites with top-layer thickness of about 1 μm.

3.3. Transport of pure solvents through PTMSP/PAN composite membranes

Besides ethanol, the optimized PTMSP/PAN composite membranes (PTMSP-3) were tested in methanol and acetone, too. Table 4 compares the solvent permeability and dye retention of PTMSP/PAN with various commercial NF polymeric membranes (hydrophilic and hydrophobic) in methanol, ethanol and acetone [30] (to recalculate the permeability in kg/(m^2 h bar) from [30], methanol, ethanol and acetone densities were used as 0.791, 0.789 and 0.791 g/cm^3, respectively). The data for PTMSP/PAN membranes are average values of at least two different membrane samples. To minimize concentration polarization effects all experiments were done at the trans-membrane pressure of 5 bar.

Table 6
Correlations between solvent permeability P^* [l/(m^2 h bar)] and the macroscopic properties of the solvents and polymer–solvent interaction.

Parameter	Methanol	Ethanol	Acetone	R^2
P^*	7.7	4.8	17.2	–
P^*/SD	18.4	7.7	32.4	0.0387
$P^* \mu$	4.2	5.2	5.2	0.9728
$P^* \nu$	52.7	65.9	65.2	0.9726
$P^* \mu/V_m$	0.10	0.09	0.07	0.9842
$P^* \nu/V_m$	1.3	1.1	0.9	0.9844
$P^* \mu$/SD	9.9	8.3	9.7	0.9949
$P^* \nu$/SD	125.4	104.6	123.0	0.9950

Table 4 shows that the methanol, ethanol or acetone permeability through PTMSP/PAN membranes significantly exceeds those of Desal-5-DK, MPF-44 and MPF-50 membranes, whereas SolSep-169 membranes seem to be the most permeable for these solvents. All membranes possess rather high rejection of two negatively charged dyes with different molecular weights – Remazol Brilliant Blue R (MW 626.5; PTMSP/PAN) and Erythrosine B (MW 880; Desal-5-DK, MPF-44, MPF-50 and SolSep-169).

In our previous work [12], it was shown that the solution-diffusion model cannot fully describe the ethanol transport through dense PTMSP membranes. It should be mentioned that gas transport through PTMSP has already been considered to be in "the transition region" between the pore-flow and the solution-diffusion [31]. Besides transport through the polymer, flow may take place through free-volume elements ("pores") with diameter of 5–10 Å. In fact; WAXS analysis shows that PTMSP samples swollen in ethanol possess some nanoscale order (d = 8.2 Å; 2Θ = 10.6°) very close to that for glassy PTMSP in the dry state (9.0 Å; 2Θ = 9.8°) [12].

To get some insight into the solvent transport mechanism, solvent permeability was normalized with various relevant solvent properties (dynamic, μ, or kinematic, ν, viscosities and molar volume V_m) as well as with the swelling degree (SD) of PTMSP in the solvent (see Table 5). Similar approach has already been used in the literature to describe the transport through various OSN membranes (MPF-50 [32] and PDMS/PAN [3,4]). Table 6 presents the normalization of permeability and the R^2 value obtained when the solvent permeability P is plotted as a function of relevant parameter. It seems that both solvent viscosity (no difference in main conclusion if one uses dynamic or kinematic viscosity due to comparable solvent density values) and membrane swelling affect solvent transport. Nevertheless, the solvent viscosity seems to be the most critical factor for the specific solvents.

4. Conclusions

In this study, composite PTMSP/PAN membranes with different top-layer thickness were prepared by casting PTMSP solution on PAN porous support. The methanol, ethanol or acetone permeability through optimized PTMSP/PAN composite membrane (top-layer of

about 0.9 μm) significantly exceeds those of some commercial NF membranes (Desal-5-DK, MPF-44 and MPF-50), while the developed membranes have quite high retention (85–90%) of negative charged dye (MW 626.5). These membranes have quite good stability with slight decrease of ethanol transport during operation period of at least 80–230 h.

For the specific solvents studied here, it seems that the solvent viscosity is the dominant factor affecting the transport through the PTMSP/PAN membranes although the membrane swelling in the solvent is important, too. The transport of various other solvents through these membranes will be aim of future work.

Acknowledgements

The authors express gratitude to Szymon Dutczak and Miriam Girones for the SEM study of PTMSP/PAN composite membranes. Alexey Volkov acknowledges to Russian Science Support Foundation.

Nomenclature

C_{if}	dye concentration in the feed (g/g)
C_{ip}	dye concentration in the permeate (g/g)
d	membrane thickness (m)
d_0	thickness of initial membrane (m)
d_s	thickness of swollen membrane (m)
J	flux through membrane (kg/m^2 h)
MW	molecular weight (g/mol)
MWCO	molecular weight cut-off (g/mol)
p	pressure (bar)
P	permeability (kg/(m^2 h bar))
P^*	permeability (l/(m^2 h bar))
r_0	radius of initial membrane (m)
r_s	radius of swollen membrane (m)
R	membrane retention (%)
SD	swelling degree
T	temperature (K)
T_g	glass-transition temperature (K)
V_m	molar volume (cm^3/mol)
λ_{max}	wavelength with maximum absorbance (nm)
$[\eta]$	intrinsic viscosity in toluene at 25 °C (dl/g)
μ	dynamic viscosity (cP)
ν	kinematic viscosity (St)

References

[1] A.G. Livingston, L. Peeva, S. Han, D. Nair, S.S. Luthra, L.S. White, L.M. Freitos dos Santos, Membrane separation in green chemical processing: solvent nanofiltration in liquid phase organic synthesis reactions, Ann. N.Y. Acad. Sci. 984 (2003) 123–141.
[2] P. Vandezande, L.E.M. Gevers, I.F.J. Vankelecom, Solvent resistant nanofiltration: separating on a molecular level, Chem. Soc. Rev. 37 (2008) 365–405.
[3] N. Stafie, D.F. Stamatialis, M. Wessling, Insight into the transport of hexane–solute systems through tailor-made composite membranes, J. Membr. Sci. 228 (2004) 103–116.
[4] N. Stafie, D.F. Stamatialis, M. Wessling, Effect of PDMS cross-linking degree on the permeation performance of PAN/PDMS composite nanofiltration membranes, Sep. Purif. Technol. 45 (2005) 220–231.
[5] L.E.M. Gevers, I.F.J. Vankelecom, P.A. Jacobs, Solvent-resistant nanofiltration with filled polydimethylsiloxane (PDMS) membranes, J. Membr. Sci. 278 (2006) 199–204.
[6] L.E.M. Gevers, S. Aldea, I.F.J. Vankelecom, P.A. Jacobs, Optimisation of a lab-scale method for preparation of composite membranes with a filled dense top-layer, J. Membr. Sci. 281 (2006) 741–746.
[7] D.F. Stamatialis, N. Stafie, K. Buadua, M. Hempenius, M. Wessling, Observations on the permeation performance of solvent resistant nanofiltration membranes, J. Membr. Sci. 279 (2006) 424–433.
[8] P.B. Kosaraju, K.K. Sirkar, Interfacially polymerized thin film composite membranes on microporous polypropylene supports for solvent-resistant nanofiltration, J. Membr. Sci. 321 (2008) 155–161.
[9] B. Van der Bruggen, J. Geens, C. Vandecasteele, Influence of organic solvents on the performance of polymeric nanofiltration membranes, Sep. Purif. Technol. 37 (2002) 783–797.
[10] Y.H. See Toh, F.W. Limb, A.G. Livingston, Polymeric membranes for nanofiltration in polar aprotic solvents, J. Membr. Sci. 301 (2007) 3–10.
[11] K. Vanherck, P. Vandezande, S.O. Aldea, I.F.J. Vankelecom, Cross-linked polyimide membranes for solvent resistant nanofiltration in aprotic solvents, J. Membr. Sci. 320 (2008) 468–476.
[12] A.V. Volkov, D.F. Stamatialis, V.S. Khotimsky, V.V. Volkov, M. Wessling, N.A. Platé, Poly[1-(trimethylsilyl)-1-propyne] as a solvent resistance nanofiltration membrane material, J. Membr. Sci. 281 (2006) 351–357.
[13] A.V. Volkov, V.S. Khotimsky, V.V. Volkov, N.A. Platé, I.F.J. Vankelecom, L.E.M. Gevers, K. De Smet, P.A. Jacobs, Non-aqueous separation: sorption in and nanofiltration through nanopores in poly(1-trimethylsilyl-1-propyne), "Euromembrane 2004" Conference, 28 September–1 October, Hamburg, Germany, 131.
[14] A.V. Volkov, V.S. Khotimsky, V.V. Parashchuk, D. Stamatialis, M. Wessling, V.V. Volkov, N.A. Platé, The method of nanofiltration separation of organic liquids, RF patent 2297975 (2007).
[15] K. Nagai, T. Masuda, T. Nakagawa, B.D. Freeman, I. Pinnau, Poly[1-(trimethylsilyl)-1-propyne] and related polymers: synthesis, properties and functions, Prog. Polym. Sci. 26 (2001) 721–798.
[16] V.S. Khotimsky, M.V. Tchirkova, E.G. Litvinova, A.I. Rebrov, G.N. Bondarenko, Poly[1-(trimethylgermyl)-1-propyne] and poly[1-(trimethylsilyl)-1-propyne] with various geometries: their synthesis and properties, J. Polym. Sci., Part A: Polym. Chem. 41 (2003) 2133–2155.
[17] K.-V. Peinemann, K. Ebert, H.G. Hicke, N. Scharnagl, Polymeric composite ultrafiltration membranes for non-aqueous applications, Environ. Progress 20 (2001) 17–22.
[18] E.S. Tarleton, J.P. Robinson, S.J. Smith, J.J.W. Na, New experimental measurements of solvent induced swelling in nanofiltration membranes, J. Membr. Sci. 261 (2005) 129–135.
[19] K. Ebert, J. Koll, M.F.J. Dijkstra, M. Eggers, Fundamental studies on the performance of a hydrophobic solvent stable membrane in non-aqueous solutions, J. Membr. Sci. 285 (2006) 75–80.
[20] A. Datta, K. Ebert, H. Plenio, Nanofiltration for homogeneous catalysis separation: soluble polymer-supported palladium catalysts for Heck, Sonogashira, and Suzuki coupling of aryl halides, Organometallics 22 (2003) 4685–4691.
[21] J.P. Robinson, E.S. Tarleton, C.R. Millington, A. Nijmeijer, Solvent flux through dense polymeric nanofiltration membranes, J. Membr. Sci. 230 (2004) 29–37.
[22] E.S. Tarleton, J.P. Robinson, C.R. Millington, A. Nijmeijer, Non-aqueous nanofiltration: solute rejection in low-polarity binary systems, J. Membr. Sci. 252 (2005) 123–131.
[23] E. Florian, M. Modesti, M. Ulbricht, Preparation and characterization of novel solvent-resistant nanofiltration composite membranes based on crosslinked polyurethanes, Ind. Eng. Chem. Res. 46 (2007) 4891–4899.
[24] C.L. Jing Jing Bi, Y. Wang, K. Kobayashi, A. Ogasawara, Yamasaki, Effect of the casting solvent on the free-volume characteristics and gas permeability of poly[1-(trimethylsilyl)-1-propyne] membranes, J. Appl. Polym. Sci. 87 (2003) 497–501.
[25] D. Gomes, S.P. Nunes, K.-V. Peinemann, Membranes for gas separation based on poly(1-trimethylsilyl-1-propyne)–silica nanocomposites, J. Membr. Sci. 246 (2005) 13–25.
[26] J. Qiu, J.-M. Zheng, K.-V. Peinemann, Gas transport properties of poly(trimethylsilylpropyne) and ethylcellulose filled with different molecular weight trimethylsilylsaccharides: impact on fractional free volume and chain mobility, Macromolecules 40 (2007) 3213–3222.
[27] Y.H. See Toh, X.X. Loh, K. Li, A. Bismarck, A.G. Livingston, In search of a standard method for the characterisation of organic solvent nanofiltration membranes, J. Membr. Sci. 291 (2007) 120–125.
[28] D.R. Machado, D. Hasson, R. Semiat, Effect of solvent properties on permeate flow through nanofiltration membranes. Part I: investigation of parameters affecting solvent flux, J. Membr. Sci. 163 (1999) 93–102.
[29] K.D. Dorkenoo, P.H. Pfromm, Accelerated physical aging of thin poly[1-(trimethylsilyl)-1-propyne] films, Macromolecules 33 (2000) 3747–3751.
[30] J. Geens, K. Boussu, C. Vandecasteele, B. Van der, Bruggen, Modelling of solute transport in non-aqueous nanofiltration, J. Membr. Sci. 281 (2006) 139–148.
[31] J.G. Wijmans, R.W. Baker, The solution-diffusion model: a review, J. Membr. Sci. 107 (1995) 1–21.
[32] I.F.J. Vankelecom, K. De Smet, L.E.M. Gevers, A. Livingston, D. Nair, S. Aerts, S. Kuypers, P.A. Jacobs, Physico-chemical interpretation of the SRNF transport mechanism for solvents through dense silicone membranes, J. Membr. Sci. 231 (2004) 99–108.